Expansion Tubes in Australia

David E. Gildfind, Richard G. Morgan and Peter A. Jacobs

1 Introduction

Hypersonics research at the University of Queensland (UQ) was set in motion by the arrival of Professor Ray Stalker in 1977. Stalker, the inventor of the free-piston driver [1], soon commenced work on a large free-piston driven reflected shock tunnel (RST), the T4 facility, funded by the Australian Research Council [2]. This facility was a larger scale development of the earlier T1, T2, and T3 machines built at the Australian National University. T4 theoretically had sufficient scale to provide the test times, stagnation pressures, and to accommodate the model sizes, required to conduct hypersonic combustion and propulsion studies, and the facility became operational in 1987 [3]. While T4 was destined to become UQ's workhorse for hypersonic flow experiments (T4 would fire its 10,000th shot in August 2008 [4]) around this same period, in the late 1980s, the new hypersonics group at UQ simultaneously began to investigate expansion tube operation. While RSTs dominated hypersonic ground testing in the 1980s and 1990s, it was always known that the stagnation of the test gas upstream of the supersonic nozzle limited them to sub-orbital flight speeds, and there remained the need for higher enthalpy ground testing capabilities.

The expansion tube concept was initially proposed by Resler and Bloxom in 1952 [5], and Trimpi [6, 7] derived the analytical framework to predict their

D.E. Gildfind (✉) · R.G. Morgan · P.A. Jacobs
Centre of Hypersonics, The University of Queensland, Brisbane 4072, QLD, Australia
e-mail: d.gildfind@uq.edu.au

R.G. Morgan
e-mail: r.morgan@uq.edu.au

P.A. Jacobs
e-mail: p.jacobs@uq.edu.au

O. Igra and F. Seiler (eds.), *Experimental Methods of Shock Wave Research*,
Shock Wave Science and Technology Reference Library 9,
DOI 10.1007/978-3-319-23745-9_13

performance. Expansion tubes could, in theory, produce a wide range of high enthalpy flow conditions [8]. As Miller and Jones notes [9] (p. 1):

> In theory, the expansion tube (so named by Trimpi) is capable of generating a wide range of hypersonic-hypervelocity flow conditions in air without being frustrated by the two principal difficulties with more conventional-type hypervelocity wind tunnels: namely, extremely high reservoir pressures and temperatures, and the problem of maintaining thermochemical equilibrium of the gas throughout the expansion in the nozzle.

Following several preliminary expansion tube studies across the US in the 1960s, including work with the 'Langley Pilot Model Expansion Tube' [9], NASA commissioned the Langley Expansion Tube/Tunnel, and in the 1970s Miller [10] conducted the first extensive experimental investigation into expansion tube operation. Miller found that for a given test gas, suitably steady test flows could only be obtained for a very narrow range of test conditions; "only a single flow condition, in terms of Mach number and Reynolds number…for a given test gas" [9] (p. 371). Many flow conditions had unacceptable levels of noise in the test flow [11], for reasons that were inexplicable at the time. Due to the relatively unsatisfactory findings of the Miller investigation, as well as "diminished programmatic needs" [9] (p. 371), the Langley Expansion Tube/Tunnel was deactivated in January 1983 [9], and the expansion tube concept lost traction in the years that followed this first phase of research activity.

Given its heritage with Professor Stalker and his free-piston driver invention, it was fitting that the UQ research group would be the first to use a free-piston driver to power an expansion tube [8]. In the late 1980s, NASA Langley contracted the UQ group to explore the possibility of driving an expansion tube with a free-piston compressor in order to produce high quality expansion tube flows. TQ, shown in Fig. 1, was a relatively small pilot facility, comprising a compression tube that was 2.3 m long with a 0.1 m diameter bore, used a 3.4 kg piston, and had a driven tube that was 5.26 m long with a 38.6 mm bore [8]. The driven tube was partitioned by a thin cellophane diaphragm into a 2.08 m long shock tube and 3.18 m acceleration tube [8]. It was thought that the 'versatility' of the free-piston driver might expand the window of useable test conditions [8].

The purposes of these initial experiments with TQ, which began in 1987 [12], were to replicate the Langley flow conditions in UQ's smaller facility, to establish if additional and acceptably steady test flows could be developed, and to investigate reasons for the poor test flows previously observed [8]. A systematic study with TQ eventually led to the discovery by Paull and Stalker [11, 13] of the cause of test

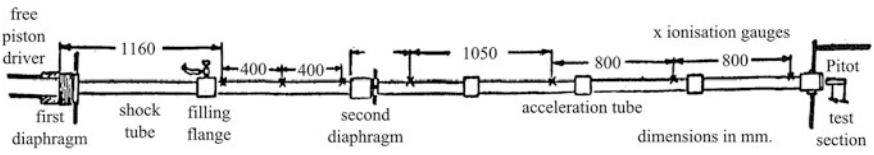

Fig. 1 Schematic of UQ's first expansion tube, TQ (adapted from [8])

flow unsteadiness (discussed later in this chapter) that had rendered so many flow conditions unusable in earlier studies. Not only did this finally explain the mechanism behind the observed test flow noise, but it also provided the means for rational flow condition design which would avoid the noise problem. Thus, faith in the potential of expansion tubes was gradually restored, and beginning with UQ, international research efforts with these facilities resumed.

This chapter provides an overview of UQ's experience with expansion tubes, which has involved four progressively larger facilities, TQ, X1 (a modification of TQ), X2, and X3. The chapter discusses the key developments at UQ, which begin with overcoming the problem of test flow noise, and finish at the present day with X3, the world's largest and highest performance free-piston driven expansion tube facility.

2 Principle of Operation

An expansion tube involves complex wave processes which are difficult to control and to measure. Referring to Fig. 2, the test gas is initially contained in a long steel tube (the shock tube), sealed at one end by a thick steel diaphragm (the primary diaphragm), and at the other end by a thin (typically) Mylar diaphragm (the secondary diaphragm). Upstream of the steel diaphragm is a larger diameter 'compression' tube, which contains a free-sliding massive piston and a light 'driver' gas such as helium; on the downstream side of the secondary diaphragm is another long

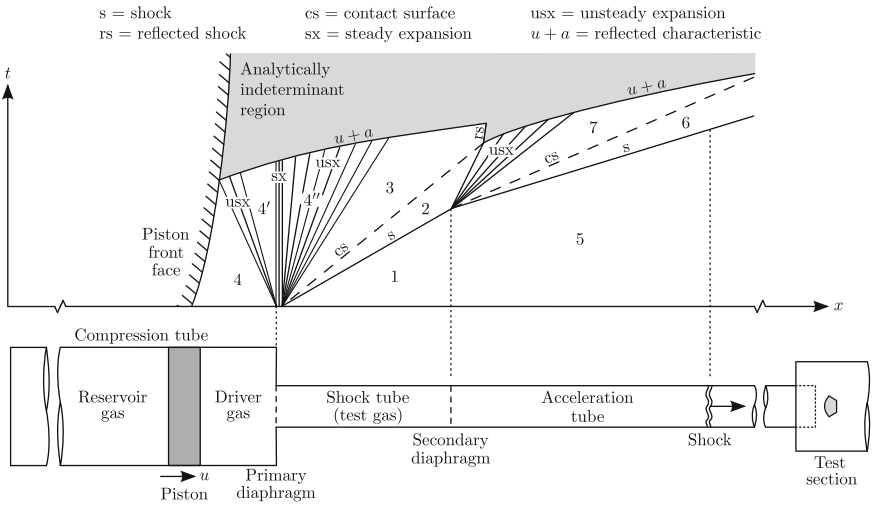

Fig. 2 Schematic diagram of a free-piston driven expansion tube (longitudinal scale greatly compressed)

tube (the acceleration tube) which extends to the test section, and initially contains air at very low pressure.

When the facility is operated, the heavy piston is fired towards the steel diaphragm, reaching maximum speeds of between 500 and 1000 km/hr. The piston compressively heats the helium driver gas in front of it, driving up the pressure and temperature until the gas explodes through the steel primary diaphragm. At the moment when the steel diaphragm ruptures, the driver gas pressure is tens of megapascals, and its temperature thousands of Kelvin. An extremely strong shock is driven into the test gas, compressing it and accelerating it down the tube. The test gas, now at high pressure and very hot, eventually arrives at the Mylar diaphragm, blasts through it, and suddenly encounters the low pressure (of order 10^0–10^2 pascals) of the downstream acceleration tube. This sudden change in boundary condition allows the test gas, already moving at several km/s, to expand forward towards the test section to speeds as high as 20 km/s.

The 'expansion tube' takes its name from this final unsteady expansion process. Total pressure and total temperature both increase when a supersonic flow undergoes an unsteady expansion. Unlike RST facilities, since the test gas is never stagnated, expansion tubes are not structurally limited by total temperature and pressure limits [14]. Furthermore, levels of dissociation and radiative losses can be minimised since the shock wave is no longer the only mechanism which adds energy to the test gas [15, 16].

The unsteady expansion process relies on the transfer of energy from the unexpanded upstream test gas to the expanded downstream test gas. Since only part of the test gas can be processed completely, test times are correspondingly reduced; "energy and total pressure are added to the flow at the expense of test time" [15] (p. 605). When the expanded test gas arrives at the test section the flow experiment begins; when the leading edge of the downstream unsteady expansion wave arrives, the test time ends. The useful test time is therefore brief, usually lasting less than one millisecond; however, expansion tubes can produce chemically clean high enthalpy test flows, and they have the highest total pressure capability currently available in a ground test facility.

3 Experience with the TQ and X1 Facilities

3.1 Test Flow Frequency Focusing

As already noted, TQ, shown in Fig. 1, was a pilot facility intended to investigate the reasons for test flow unsteadiness observed in previous studies (for example, [17–20]). Paull and Stalker [11] made the distinction between 'high enthalpy' and 'low enthalpy' flow conditions; high enthalpy test flows had acceptable quality test flows, low enthalpy test flows did not. They performed a theoretical analysis of an acoustic wave as it traverses an unsteady expansion [13], and proposed that the

unsteady expansion at the secondary diaphragm, which produces a large drop in the sound speed of the test gas, has the effect of focusing all frequency components of noise present in the test gas into a narrow bandwidth of frequencies [11]. This is later characterised as strong disturbances in the test flow. It was also shown that this focusing effect only occurs for lateral acoustic waves (radial waves in an axisymmetric facility); the effect does not occur for longitudinal waves. Numerical simulations of the full Langley expansion tube [21] also showed radial disturbances from the tube area change at the primary diaphragm station focusing into a radial wave train that propagated into the expanded test gas.

This frequency focusing effect is an inherent feature of the unsteady expansion process, and occurs for both high and low enthalpy flow conditions. The reason that high enthalpy flow conditions have acceptable test flow quality is because for these conditions the test gas has very low levels of noise *prior* to the unsteady expansion, so that even after frequency focusing has occurred, noise levels remain acceptably low. In contrast, low enthalpy flows typically already have high levels of noise in the test gas prior to the unsteady expansion, and after frequency focusing these disturbances become unacceptably large. The characteristic difference between these two types of flows is the relative ratio between the sound speeds of the shock processed test gas, a_2, and the expanded driver gas, a_3 (refer to Fig. 2 for designation of gas regions).

Paull and Stalker determined that operating an expansion tube in a suitably over-tailored configuration (i.e. $a_2 > a_3$ in Fig. 2) can prevent acoustic disturbances present in the expanded driver gas from penetrating the test gas, the effect being likened to an 'acoustic buffer' [11]. The required ratio a_2/a_3 increases where higher frequency noise is to be suppressed, or where the driver gas sound speed is lower. Neely et al. [22] applied these principles to the TQ facility, successfully demonstrating steady air and argon test flows at flow velocities up to 9 km/s. In practice, Paull and Stalker [11] indicate that an acoustic buffer will be effective for $a_2/a_3 > 1.25$. This ratio is also supported by Morgan [15], which was published several years later following greater experience with the concept.

Paull and Stalker concluded that successful expansion tube operation would be limited to high enthalpy conditions (where the shock-processed test gas is very hot and therefore has a high sound speed) unless some means of reducing the noise in the driver gas could be devised. This seemed unlikely in a free-piston driven expansion tube; aside from the diaphragm rupture process itself, the expansion of driver gas through the area change has been shown to be a fundamental source of radial disturbances [23]. However, Morgan [15] would later propose that this sound speed increase could instead be achieved by using a shock-heated helium secondary driver, thus dramatically expanding the useful operating range of these facilities.

3.2 Operation with a Shock-Heated Secondary Driver

Henshall [24] first proposed the concept of a shock-heated secondary driver, and Stalker and Plumb [25] were the first to experimentally verify it (using a standard shock tube arrangement). Operation with a secondary driver involves placing a volume of, typically, helium between the primary diaphragm and the test gas. Referring to Fig. 3, the secondary driver is operated in the over-tailored mode such that $a_{sd2} > a_{sd3}$; i.e. the expanded primary driver gas (Region *sd*3) has a lower sound speed than the shock-processed secondary driver helium gas (Region *sd*2).

When a secondary driver is used, the shock-processed helium becomes the driver for the test gas. Observing Fig. 3, the pressure and velocity are constant across the *sd*2/*sd*3 interface. The extent of compressive shock heating which the Region *sd*2 gas undergoes, and therefore its temperature and sound speed, depends on its initial fill pressure. At sufficiently low fill pressures, the helium gas will be compressively heated so much that its temperature far exceeds the temperature of driver gas which could otherwise be achieved by free-piston compression alone. With a sufficiently high sound speed, the Region *sd*2 gas can potentially drive a faster shock through the test gas than the primary driver would be able to by itself.

The benefit of the secondary driver comes at the expense of duration, since the region *sd*2 gas expands more rapidly by virtue of its higher sound speed, although this may not be a concern for high enthalpy conditions. Furthermore, for a given total driven tube length, the secondary driver reduces the length of the remaining

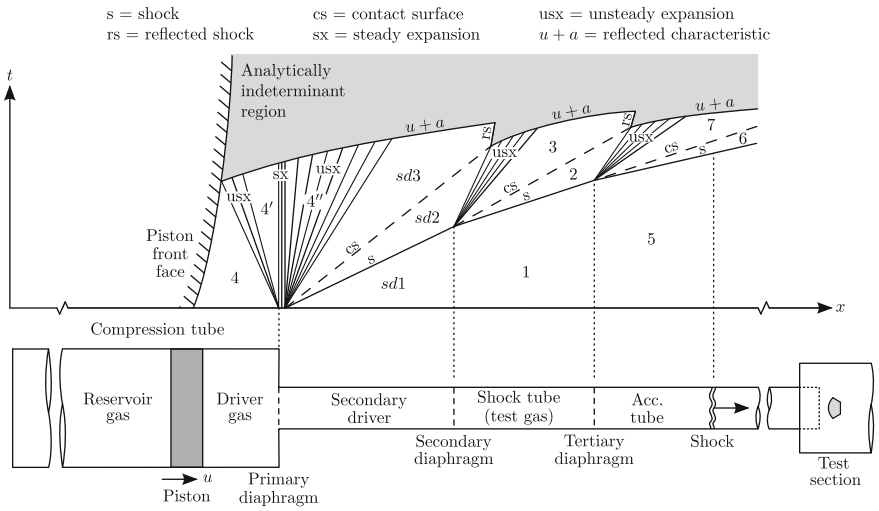

Fig. 3 Schematic diagram of wave processes occurring inside a free-piston driven expansion tube with shock-heated secondary driver (longitudinal scale greatly compressed). An *unsteady expansion* is assumed to form at the secondary diaphragm, which is typical for super-orbital operation of these facilities where the test gas is initially at low density

tubes, increases the complexity of internal flow processes, and adds to the amount of contaminants and debris in the flow (due to the addition of another diaphragm) [26].

Morgan and Stalker [27] first used a secondary driver with the X1 expansion tube in order to boost its super-orbital performance, and in the process achieved maximum shock speeds of 18.7 km/s. Neely and Morgan [28] further developed the "superorbital expansion tube concept", developing and characterizing a 13 km/s test flow in X1. This work also examined the influence of real gas effects and diaphragm rupture on expansion tube flow processes. Morgan [15] discusses the secondary driver concept in more detail, and details the operating regimes where this configuration can be beneficial.

As noted in the Sect. 3.1, a secondary driver can also be beneficial for lower enthalpy conditions. After Paull and Stalker [11] determined that under-tailored operation was the cause of noise transmission to the driver gas at lower enthalpy conditions, it was thought that adequate test flow quality could not be achieved at these conditions, since there was no acoustic buffer available to filter the driver noise. However, Morgan [15] later suggested that a secondary driver could be used as an alternative upstream means by which to achieve the required 'acoustic buffer', and this has subsequently opened up a much larger range of available test conditions with respect to the acoustic buffer requirement.

A couple of observations can be made about the use of a secondary driver as an acoustic buffer for low enthalpy conditions. Firstly, there is no acoustic buffer shielding the test gas from noise in the secondary driver gas, so disturbances introduced to the Region 3 gas (i.e. by Mylar diaphragm rupture, or during transit down the tube) would not be suppressed in the test gas (Region 2). Since the test gas itself lacks the intrinsic mechanism to prevent noise ingress, it would be expected that these conditions should be somewhat noisier than conditions where the test gas itself provides the acoustic buffer; without making any conclusive observations here, this does indeed reflect anecdotal experience with testing in X2 at high enthalpies with and without secondary drivers.

Secondly, while maximizing the ratio a_{sd2}/a_{sd3} may theoretically minimize noise transmission from the primary driver to secondary driver gases, this will also reduce the ratio a_2/a_3, which will increase noise transmission from the secondary driver gas to test gas. The optimum secondary driver configuration may be one which has sufficient sound speed to act as an acoustic buffer, but no more than this, although this question requires further investigation.

Finally, the critical wave processes associated with many low enthalpy conditions can be characteristically different to those associated with high enthalpy conditions. Observing Fig. 4, for sufficiently high initial test gas densities, the shock-processed secondary driver gas (Region *sd*2) will decelerate as it impacts the dense test gas (Region 1), and consequently will be compressively heated. This deceleration and compression occur due to a reflected shock (labeled 'rs' in Fig. 4) which arises at the secondary diaphragm (as opposed to the unsteady expansion shown in Fig. 3). The effect of this reflected shock on noise transmission may also require further investigation.

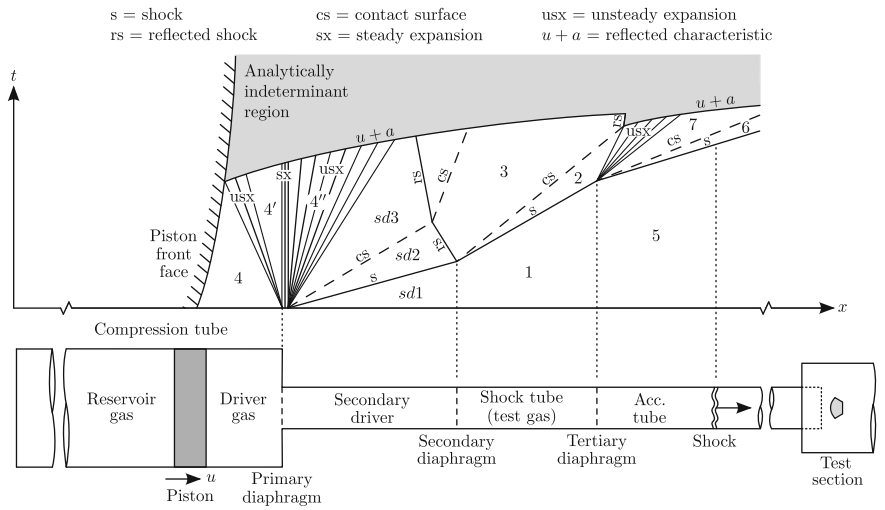

Fig. 4 Schematic diagram of wave processes occurring inside a free-piston driven expansion tube with shock-heated secondary driver (longitudinal scale greatly compressed). A *reflected shock* is assumed to form at the secondary diaphragm, which is typical for super-orbital operation of these facilities where the test gas is initially at high density

4 The X2 Facility

During the 1990s, Morgan [26] received Australian Research Council support to develop two larger expansion tube facilities, X2 and X3, which had total lengths of approximately 25 and 65 m respectively. Size is paramount for impulse facilities: a larger tube diameter permits testing of larger models; a longer tube provides a longer slug of test gas, and therefore more test time. The practical implications of increasing the facility scale become evident in Fig. 5, which compares UQ's three expansion tube facilities, beginning with TQ/X1. Despite the success of the pilot studies in TQ/X1, the driven tube bore was only Ø38 mm, and the test time was very short (for example, 15 µs of test time for a 13 km/s air condition [28]). Having established proof-of-concept with this pilot facility, the logical next step was to move to larger facilities.

X2 and X3 are each world-class facilities in their own right, however their development over the years has been strongly intertwined. X2 is a medium-sized machine which is manageable at a 'human' scale, and as such is a convenient and economical platform to trial new technologies and ideas. X3 is a much larger and heavier machine. Mechanical assistance is required to operate X3, design changes are more costly and difficult to incorporate, however this is the inevitable price to pay for X3's much higher performance. In this context, it is natural that the evolution of X2 has always been in advance of X3, and that X2 has been the initial platform for UQ's major developments with expansion tube facilities. This section focusses on X2, originally commissioned in 1995 [29], and discusses the major developments which have been accomplished with the facility.

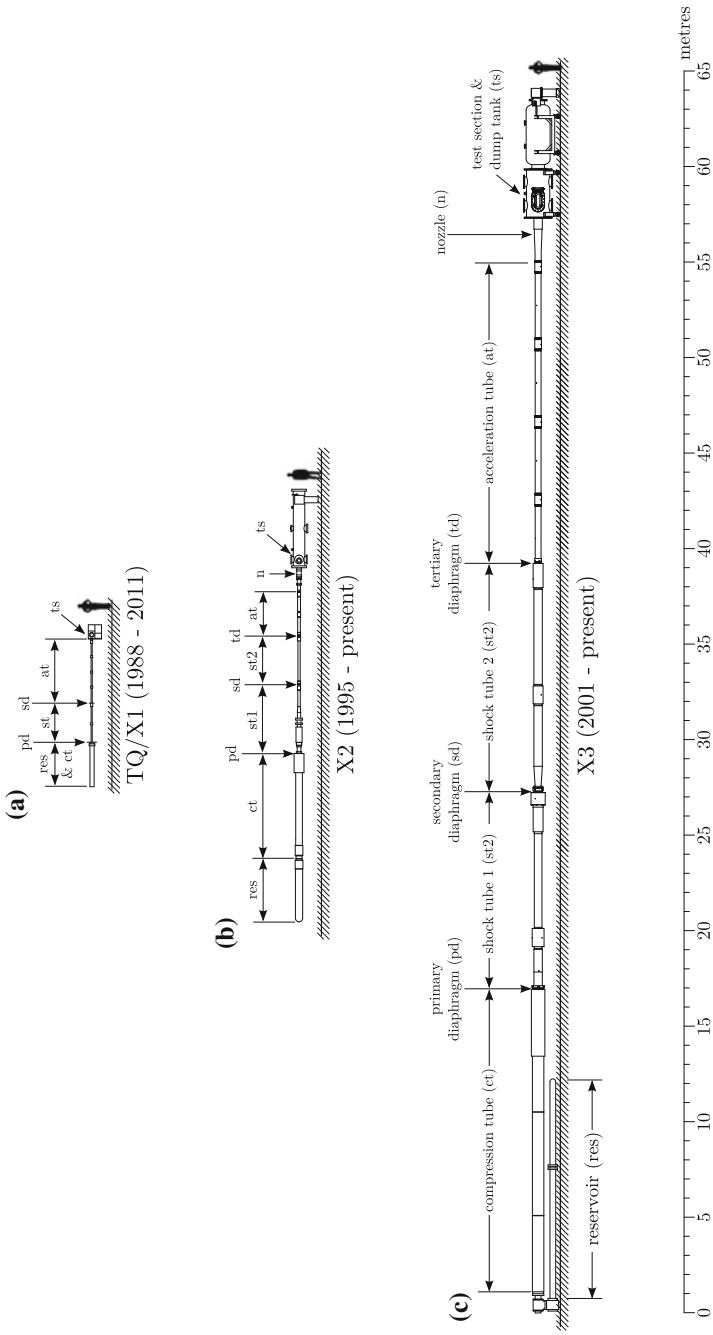

Fig. 5 The University of Queensland's X-series expansion tube facilities (to scale). Supporting carriage work, pressure manifold, and associated hardware, not shown

4.1 X2's Free-Piston Drivers

The free-piston driver is the engine which powers UQ's expansion tubes, and its performance and operating characteristics influence many aspects of the overall facility performance. X2 was originally configured with a compound driver in order to act as a prototype for the larger X3 expansion tube. Due to the size of X3, a single stage free-piston driver was considered at the time to be too expensive, so the compound piston was proposed in order to reduce costs [29, 30] (see Fig. 6). X2's two-stage (compound) free-piston driver consisted of a light aluminium outer piston, which carried a heavy stainless steel inner piston.

The first stage of the compression involves both inner and outer pistons. This stage takes advantage of the fact that for most of the piston cycle there is little compression of the gas, therefore stress levels in the first stage are low, and the structure can be lighter and correspondingly cheaper [30]. The outer piston is light, and most of the reservoir gas energy in this stage is transferred into kinetic energy in the heavier inner piston [31]. When the two stage piston reaches the buffer, the outer piston is stopped, and the inner piston continues the compression to the final primary diaphragm burst pressure [30].

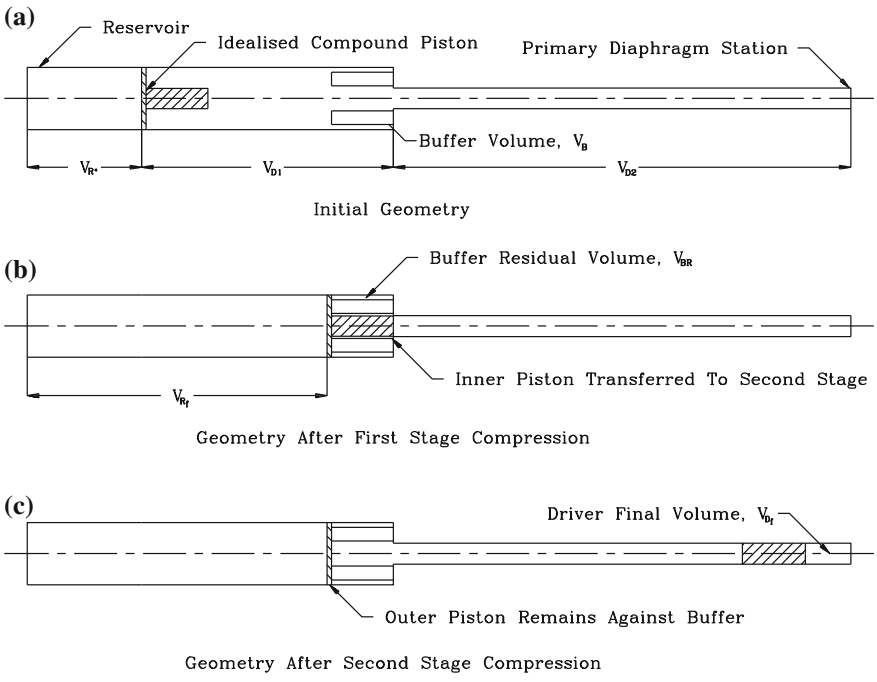

Fig. 6 Schematic of compound driver concept (reproduced from Doolan and Morgan [30])

The advantage of the compound driver is that it can achieve similar compression ratios to a single piston driver, but with a much shorter compression tube (for an inner/outer piston diameter ratio of 2, compression tube length can be reduced by approximately 75 %). Furthermore, the large diameter section of the compression tube can be made of thinner steel, since it does not have to contain the large pressures which arise at the primary diaphragm. Studies using X2's compound driver included holographic interferometry measurements of flow over cylinders [32] and flow over toroidal ballutes [33], flow tagging velocimetry [34], boundary layer development over flat plates [35], and hypersonic shock standoff on blunt bodies in ionizing flows [36].

The compound piston driver has three distinct disadvantages as compared to the single piston driver. Firstly, it is a more complicated device to operate [29]. Secondly, without the area change of the single piston, a longer slug of driver gas is required for adequate test time. Thirdly, there is a reduction in the maximum pressures and densities which can be achieved [29]. For these reasons, X2 was subsequently reconfigured with a single stage 35 kg piston, with an area ratio of 9 across the primary diaphragm. The installation of the new driver was completed in April 2004 [29].

The 35 kg piston was operated successfully for a range of flow conditions (studies included measurements of Mars entry radiation [37] and Titan entry radiation [38, 39], and Mach 10 scramjet combustion [40]). In 2009, attempts were made to simulate Mach 13 scramjet flight, but at much higher total pressures than the earlier Mach 10 scramjet combustion study [41]. It was found that the target test condition could not be achieved due to significant attenuation of the shock speed down the driven tube [41]. Figure 7 shows the primary shock speed along X2's driven tube. The dashed lines show the required shock speeds to achieve the Mach 13 condition; the data points show the experimentally measured shock speeds between adjacent pressure transducers located in the tube wall; the solid curve shows a later computation of the shock speed using the 1-D Lagrangian CFD code, L1d [42].

Referring to Fig. 7, strong rarefaction waves originating at the free-piston driver were responsible for the significant shock speed attenuation. Initial flow condition

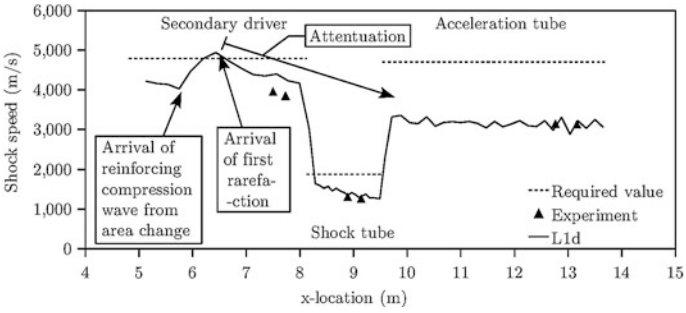

Fig. 7 Shock speed versus position for Mach 13 flow condition, using 35 kg piston with 100 % helium driver (reproduced from Gildfind et al. [41]). Primary diaphragm is located at x = 4.810 m. Maximum experimental uncertainty is ±3 %

calculations had used analytical methods which did not take into account transient wave processes in the driver; subsequent analysis with L1d, which included the full piston dynamics, indicated that the observed attenuation was due to rapid expansion of the driver gas following diaphragm rupture [41].

The 35 kg piston is relatively heavy compared with the length of X2's driver (4.5 m), and as a consequence, it is operated relatively slowly (speed is less than 100 m/s when the diaphragm ruptures). The results in Fig. 7 are for a 100 % helium driver gas operating at a compression ratio $\lambda = 42$. At this condition, the driver gas volume is small when rupture occurs, and the compressed helium is hot and therefore has a very high sound speed. The slow moving piston presents an approximately static boundary in comparison to the timescales associated with the unsteady expansion of the driver gas. This unsteady expansion soon reflects off the piston face, and is transmitted downstream as a $u + a$ wave. For higher enthalpy flow conditions, critical flow processes traverse the tube before this relaxation catches up. However, high total pressure scramjet flow conditions, which involve generating slower shock speeds (1–2 km/s) through much denser test gases, take longer to traverse the tube. At these lower enthalpy, higher total pressure conditions, the driver pressure relaxation must be delayed or else it will interfere with critical flow processes, as observed in Fig. 7 (see 'Arrival of first rarefaction').

One method to increase the useful driver gas supply time is to operate a 'tuned' free-piston driver [43]. This involves running the piston at sufficiently high speed, so that when the primary diaphragm ruptures, the piston displacement compensates for driver gas loss to the driven tube [41]. In practice the piston is run even faster than this—it is 'over-driven' [44]—such that even after the diaphragm ruptures, the driver pressure momentarily continues to increase. The piston, which is rapidly decelerating during this process, eventually slows to the point that the driver pressure drops. This process can, however, significantly extend the duration of time over which the driver gas is maintained at high levels.

The challenge with tuned operation in X2 was to be able to first accelerate the piston to high speeds (of order 200–250 m/s for X2), and then bring it to a soft landing at the other end of the tube, all within X2's 4.5 m compression tube length. Analysis indicated that the piston would have to be as light as possible, and a new 10.5 kg piston was developed. The piston, shown in Fig. 8, is manufactured from 7075-T6 alloy, was designed to sustain a maximum deceleration of approximately 40,000 g before ultimate failure (80 MPa driver pressure), and can be routinely operated up to approximately 20,000 g (40 MPa driver pressure).

The effect of tuned operation is shown in Fig. 9 (note: tuned conditions in Fig. 9 are given the designation 'x2-LWP-#.#mm-0', where #.# indicates the steel diaphragm thickness). The black and green traces show computed driver pressures for tuned operation of the 10.5 kg piston, and nominal operation of the 35 kg piston, respectively. Both of these conditions use a 1.2 mm thick steel primary diaphragm, with a nominal rupture pressure of 15.5 MPa. The blue and red curves show computed driver pressures for tuned operation with 2.0 and 2.5 mm thick diaphragms. It can be seen that tuned operation significantly changes the characteristics of the driver pressure trace.

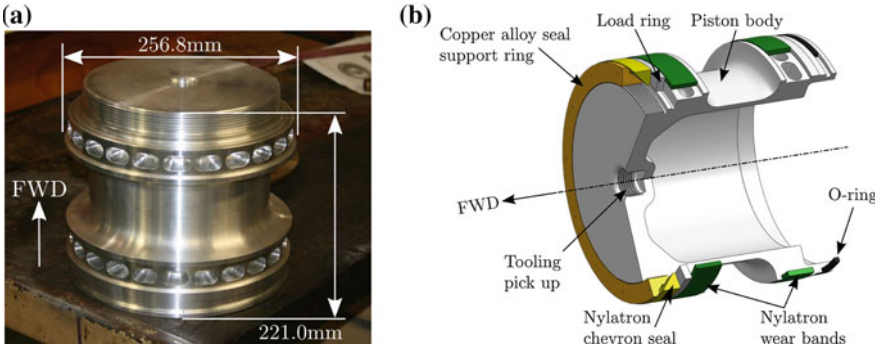

Fig. 8 X2's lightweight 10.5 kg piston. **a** Piston body, machined from 7075-T6. **b** Cutaway view of piston assembly. Adapted from Gildfind et al. [41]

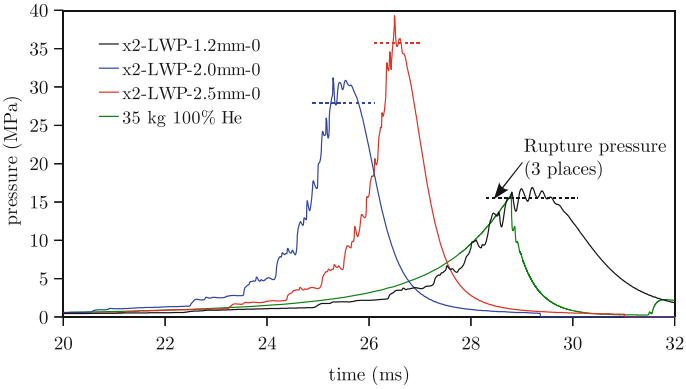

Fig. 9 L1d computed driver pressures. Driver pressure for 35 kg piston is shown for comparison (*green curve*); this pressure history has been time-referenced to align its rupture time with driver condition X2-LWP-1.2 mm-0 (both use the same 1.2 mm thick diaphragm, with nominal 15.5 MPa rupture pressure). Reproduced from Gildfind et al. [41]

Considering the black and green traces (for the 1.2 mm diaphragm), while it can be seen that tuned operation sustains the driver gas pressure for an order of magnitude longer duration, the tuned condition (black curve) has a lower compression ratio ($\lambda = 17.5$ compared to $\lambda = 42$), and uses a heavier driver gas (80 % He/20 % Ar compared to 100 % He), and therefore cannot drive the same *initial* shock speed as the 35 kg piston condition (green curve). However, operation of the tuned driver at higher diaphragm rupture pressures (the blue and red curves), and correspondingly higher compression ratios, achieves similar initial performance to the 35 kg piston condition, and furthermore, demonstrates no attenuation. The required, computed and experimental shock speeds for driver condition 'x2-LWP-2.5 mm-0' in Fig. 9 are shown in Fig. 10. It can be seen that experimental shock speeds are within 10 % of the required shock speeds, with no obvious attenuation.

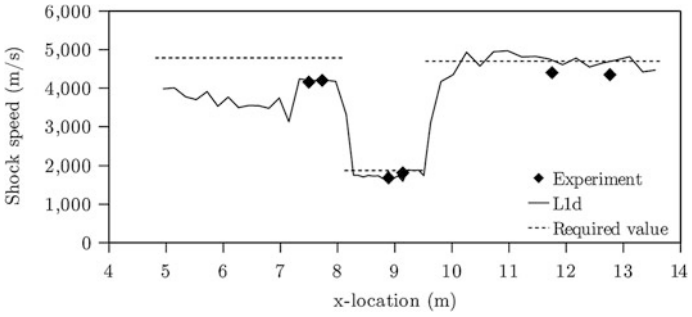

Fig. 10 Comparison between experimental and computed shock speeds for X2 tuned driver condition X2-LWP-2.5 mm-0 (reproduced from Gildfind et al. [41]). Maximum experimental uncertainty is ±2 %. No shock attenuation is observed

For driver condition X2-LWP-2.5 mm-0, the peak deceleration of the 10.5 kg piston is computed to be 17,957 g, which is approximately 3 times higher than the next comparable facility, T5 in Caltech [41]. This demonstrated that using a very light piston makes it possible to use a relatively short compression tube to achieve a level of driver performance approaching that of much larger international facilities.

The 10.5 kg piston was successfully used to generate the scramjet test flows for which it was designed, achieving test flows between Mach 10 and 14, at a maximum total pressure of 10.4 GPa [45]. The tuned driver is now in routine use in X2, and has since been used for studies of Titan gas emission spectroscopy [46], VUV spectroscopy of Earth re-entry flows [47], carbon hot wall reentry testing [48], and simulation of gas giant entry radiation [49]. To achieve very high enthalpy conditions (such as 11.5 km/s Earth re-entry), higher fractions of helium are required for the driver gas. This is achieved through the use of orifice plates at the driver area change [50], which reduce the choked diameter at the area change, and are sized to achieve the same volumetric flow rate as the original driver operating condition, thus ensuring that piston dynamics are preserved.

4.2 X2 Mach 10 Nozzle

Considering a facility such as X2, the basic core flow is constrained to be less than the diameter of the driven tube (Ø85 mm for X2), and significantly less when boundary layers are accounted for. The purpose of using a contoured nozzle is primarily to increase the test gas core flow size, although the test time may also increase slightly [51, 52]. Hypersonic nozzles are characterised by being purely diverging, with fully hypersonic flow throughout [53].

A steady expansion nozzle increases the size of model which can be tested, which has practical benefits in terms of model size and instrumentation. Increasing model size does not assist with meeting binary scaling (ρ-L) targets, since the

Fig. 11 The X2 Mach 10 nozzle (reproduced from Scott [54])

corresponding reduction in test flow density (approximately proportional to D^2) is greater than the increase in model size (proportional to D). However, due to the very high levels of total pressure achievable, the reduction of this ρ-L term due to nozzle expansion can often be compensated.

X2 has a contoured steel nozzle which is full capture and shock free [54]. The preliminary design of the nozzle used the method of characteristics, targeting an exit flow Mach number of 10 for an inflow Mach number of 7.3, and a 0° flow angle, assuming inviscid and irrotational flow [54]. This shape was then further optimised using a Nelder-Mead technique matched with the compressible flow solver SM_3D+ [55]. The nozzle, shown in Fig. 11, was tested by Scott [54] for three conditions (two air and one Titan atmosphere) and found to produce acceptable results.

The difficulty with contoured nozzles is that they are optimised for a single nozzle inlet Mach profile. Whilst the contoured nozzle may produce a uniform exit flow at the design Mach number, it is more susceptible to flow non-uniformities at off-design conditions [53]. Furthermore, these nozzles are susceptible to shock generation by the wall contour, and the high Mach numbers through the nozzle encourage growth of boundary layers, which may already be thick at the acceleration tube exit/nozzle inlet [53].

Scott's [54] nozzle design process accounted for the presence of boundary layers with its second stage SM_3D+ analysis, however it is noted that this applies to a steady inflow, whereas actual expansion tube inflows are transient. This optimisation process also required an inflow Reynolds number to be selected, therefore deviation from this Reynolds number during operation also constitutes an off-design condition.

For idealised supersonic flow in a diverging nozzle, the Mach number depends only on cross-sectional area, and is calculated by solving Eq. (1), where the subscripts i and o indicate nozzle *inflow* and *outflow* respectively. If Eq. (1) is used with the *geometric* area ratio, A_o/A_i, it will often over-predict the flow expansion in comparison to experiment, since thick and varying boundary layers will affect the *actual* area change of the test gas *core flow*. Instead, an *effective* area ratio is used, and experience with X2 indicates that this can only be established from a combination of experimentation and sophisticated CFD analysis (refer Sect. 4.3.2).

$$\frac{M_i}{M_o}\left[\frac{1+\frac{\gamma-1}{2}M_o^2}{1+\frac{\gamma-1}{2}M_i^2}\right]^{\frac{(\gamma+1)}{2(\gamma-1)}}=\frac{A_o}{A_i} \tag{1}$$

4.3 Test Flow Characterisation

Test flow characterisation involves quantifying relevant test flow properties. For an expansion tube these include:

- Static pressure, temperature, and velocity;
- Core flow diameter (the portion of steady flow across the nozzle exit plane which is not excessively affected by boundary layer effects). Pitot pressure measurements are typically used to establish the size of this region;
- The steadiness or unsteadiness of these properties as the test time progresses;
- Shock speed is measured since it provides critical information about primary wave processes before test flow arrival at the test section;
- Chemical and thermal composition of the test flow: levels of vibrational excitation and thermal nonequilibrium become increasingly important at the upper envelope of planetary entry flows and scramjet combustion.

In an expansion tube, it is exceedingly difficult to measure these flow properties directly, especially with intrusive instrumentation. For example, while it is possible to directly measure the static pressure along the tube wall, it is not possible to directly measure this property away from the wall without first interfering with the flow itself. Furthermore, the expansion tube presents an extremely harsh instrumentation environment. A probe placed in the path of an expansion tube flow is subject to the extreme heating of hypervelocity flow, and is impacted by debris which trail behind the test gas. Referring to Fig. 12, the Mylar film, initially used to separate gases in the driven tube, later becomes entrained in the flow as particulates; these particulates arrive after the test gas and act as hypersonic projectiles, potentially impacting and damaging sensitive hardware in the test section. To protect expensive pressure transducers they are shielded from the flow, but this significantly complicates their aerodynamic response, and can reduce their sensitivity and degrade their measurement.

The experimenter is therefore presented with only a limited range of direct and indirect measurements. CFD models of expansion tube flow processes are then used to build a more complete picture of the flow (i.e. to fully characterise it). CFD has progressed to the point that it is now routinely used to perform ‘virtual’ experiments for comparison with ‘actual’ experiments. These simulations fully characterise the flow, however the utility of these calculations depends on how well they correlate with experimental measurements. The codes continually evolve to include more detailed physical models, and are calculated with greater resolution. The critical limitation however is that the uncertainty in CFD calculations is directly dependent

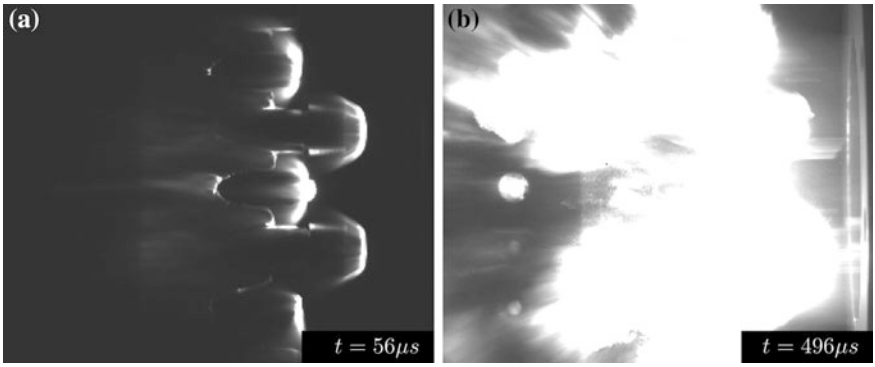

Fig. 12 High speed camera footage of flow in X2 (adapted from Gildfind [56]). **a** Test gas flowing from *right* to *left* over Pitot probes. **b** Later arrival of driver gas and entrained particulates

on the uncertainty in experimental measurements. Improving characterisation of expansion tube test flows therefore relies on the simultaneous improvement of both experimental and numerical techniques.

4.3.1 Test Flow Measurements

Experimental pressure measurements are used for routine characterisation of the test flow. Figure 13 shows the layout of piezoelectric PCB static pressure transducers along the length of X2, as well as other leading dimensions. These transducers are positioned in the tunnel wall, flush with the internal surface of the tube, and measure the static pressure of the flow as it passes. The microsecond response time of the gauges permits accurate identification of the time of shock arrival, and this data is used to calculate the average time of flight of the shock between adjacent transducer pairs. These measurements therefore provide experimental data about the static pressure of the flow, as well as the shock speed, and are an important diagnostic tool for reconstruction of the test flow properties.

The core flow is determined by sampling Pitot pressure across the tube exit. As discussed in Sect. 4.3 (and Fig. 12) the expansion tube presents an extremely harsh instrumentation environment, particularly for direct measurements of Pitot pressure. When pressure transducers are used, protective caps are utilised to prevent line-of-sight to the transducer sensing surface. Figure 14 shows various techniques used to protect transducers during Pitot pressure measurements. Figure 14a shows a standard Pitot cap, which has an internal brass diffuser to block line-of-sight of the flow to the internal transducer. Figure 14b and c show two variations of swirl cap which have four vortically aligned holes feeding the cavity containing the PCB sensing surface; these holes are designed to induce swirl in the flow, which is intended to dampen Helmholtz Resonance inside the Pitot cavity [57]. Even with

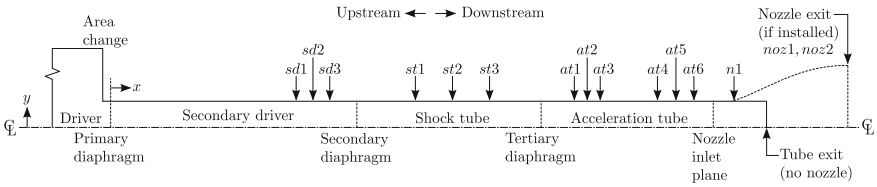

Description	x (mm)	y (mm)
Piston front face prior to launch	$-4,589$	-
Driver area change	-110	-
Primary diaphragm downstream face	0	-
Transducer $sd1$	2,577	42.5
Transducer $sd2$	2,810	42.5
Transducer $sd3$	3,043	42.5
Secondary diaphragm downstream face	3,418	-
Transducer $st1$	4,231	42.5
Transducer $st2$	4,746	42.5
Transducer $st3$	5,260	42.5
Tertiary diaphragm downstream face	5,976	-

Description	x (mm)	y (mm)
Transducer $at1$	6,437	42.5
Transducer $at2$	6,615	42.5
Transducer $at3$	6,796	42.5
Transducer $at4$	7,590	42.5
Transducer $at5$	7,846	42.5
Transducer $at6$	8,096	42.5
Nozzle inlet plane	8,343	-
Transducer $n1$	8,652	42.5
Tube exit (no nozzle)	9,105	42.5
Nozzle exit (if installed), $noz1, noz2$	10,731	100.8

Fig. 13 Schematic diagram of X2's experimental setup. Horizontal scale has been compressed for clarity. Free-piston driver is not shown. Location of the exit plane for configurations with and without the Mach 10 nozzle are shown

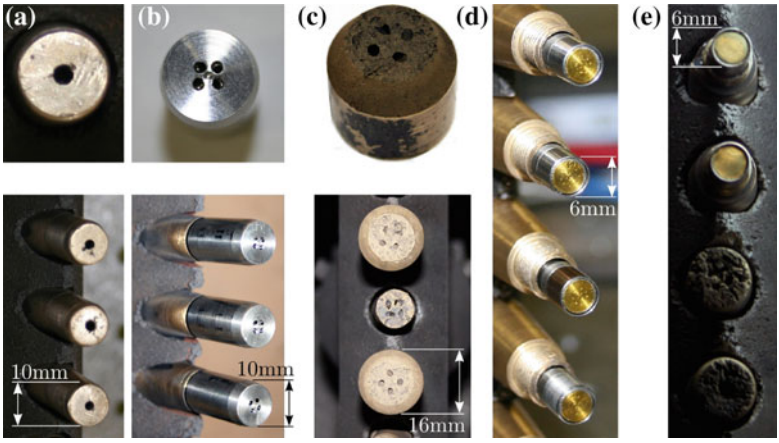

Fig. 14 Various Pitot probe configurations. **a** Standard brass single hole cap (used with an internal brass six hole impact plate to prevent line-of-sight between flow and the PCB transducer face). **b** Stainless steel 4 hole swirl cap. **c** Brass T4 RST 4 hole swirl cap (vibration isolated with rubber). **d** Example of cellophane protection across PCB transducer face. **e** Example of 0.05 mm thick brass shim protection across PCB transducer face

these shielding techniques, the internal cavity can still get extremely hot; Fig. 14d and e respectively show examples of cellophane and brass shim being applied to the PCB sensor surface to protect the transducer from the high transient heat loads.

A recent study in X2 [45] to develop scramjet flow conditions, with total pressures in the gigapascal range, found that normal Pitot measurement techniques, such as those detailed in Fig. 14, could not produce meaningful pressure measurements. These flow conditions induce high heat loads on the Pitot probe caps, and have large amounts of entrained Mylar since these diaphragms must be relatively thick to contain the high initial fill pressure (typically 0.1–0.2 mm Mylar thickness). A combination of brass shim and Pitot swirl cap was required to prevent transducer damage, after which the response became inadequate. While this combination has been used with RST facilities, the test times in X2 are much shorter (of order 100 μs, compared to order 1000 μs), and the increase in response time becomes prohibitive.

In order to reduce the Pitot transducer heat loads, a conical probe was designed based on a 15° half angle, using eight holes to fill the sensor cavity, as shown in Fig. 15. Whereas a Pitot probe measures the stagnation pressure behind a normal shock, the cone probe processes the flow with a conical shock. The static pressure at the cone surface still provides information about the flow density and velocity, however, the flow over the cone probe is significantly less severe, and each cone's pointed tip presents a smaller obstacle to oncoming debris entrained in the flow. Initial experimentation with these probes has provided promising initial results [45], however UQ is still establishing their full performance characteristics.

Finally, UQ has also measured Pitot pressure using bar gauges [58] (Fig. 16). A strain-gauged bar is placed into the flow, and the strain gauge response over time is measured. The flow is processed by a normal shock which forms over the disc at the exposed end of the bar; the average pressure in the bar cross-section can be

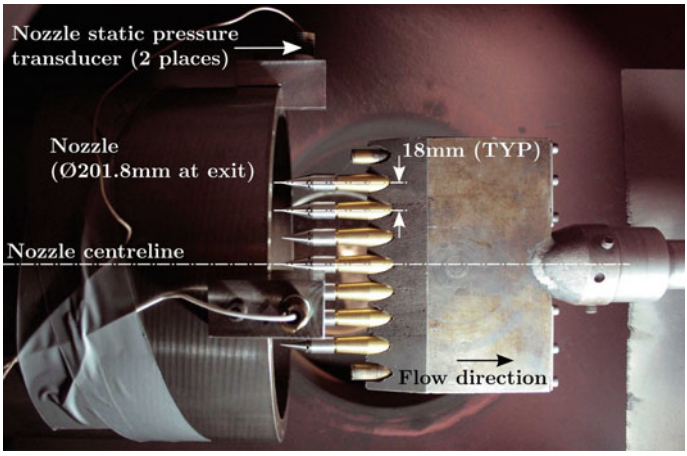

Fig. 15 Conical probe arrangement in test section, X2 with nozzle

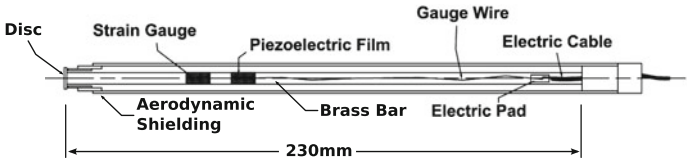

Fig. 16 Schematic of stress wave bar gauge (adapted from [58, 59])

closely correlated to the aerodynamic pressure acting on the disc at the stagnation streamline (i.e. the Pitot pressure). When the flow impacts the disc, stress waves are propagated down the bar. The bar is long and thin, so the stress waves are approximately planar. An axial strain measurement on the *surface* of the bar therefore provides a measurement of the axial strain *through* the bar, which can be used to calculate the axial force. Unless de-convolution techniques are used, this approach can provide a force measurement up until the stress waves reflect from the other end of the bar and return to the strain gauge. Chiu and Mee [58] report a rise time of approximately 5 μs, an uncertainty of ±7 %, and test times of 100 μs for a 230 mm long bar. This level of performance comes at the cost of complexity, durability, and test time however, and as a result these gauges have not been used for routine measurements in UQ.

4.3.2 Facility Numerical Simulation

UQ, with its extensive and long term experience with expansion tubes, has been involved in the majority of axisymmetric simulation work on these machines. These simulations have been performed with several purposes in mind:

1. *To fully characterise the test flow*. The process of experimentally characterising expansion tube test flows is very challenging, primarily due to short test times, harsh environmental conditions, space restrictions, and a lack of available non-invasive diagnostic techniques to make direct measurements. The advanced measurement techniques which *are* available, are correspondingly expensive, however even the most advanced equipment can only reveal a small portion of the flow properties, and typically only at a few spatial locations.
2. *Development of new flow conditions*. Axisymmetric CFD is the most accurate of the *practical* tools available to predict facility response for new flow conditions. Obtaining a good estimate of the facility response permits many potential issues to be addressed prior to conducting an experimental campaign (which can be costly and is usually time constrained). Once benchmarked against an existing flow condition experiment, the code can then be used for parametric design studies to improve or modify that flow condition. However, despite the utility of these codes, the experiment itself remains essential in order to establish the *actual* flow. The further away from the benchmarked conditions which the code

departs, the less reliable must the computed solution be assumed to be, and correspondingly greater care must be applied to its predictions.

3. *Validation of numerical codes.* Numerical codes need to be validated against experimental results, particularly in the hypersonic flight regime [60–65]. Validation data may comprise, for example, pressure or heat transfer measurements on the surface of a model in the test section, Pitot pressure measurements from a probe located in the path of the test flow, spectroradiometric measurements of the flow through an observation window into the test section, and so forth. A similar 'numerical experiment' is then performed, and the computed flow properties are compared to the experimental measurements. In order to accurately repeat the 'numerical experiment', it is typically necessary to first simulate part or all of the facility flow processes upstream of the test section, so that the complex transient test flow is accurately reproduced. To otherwise assume that the test flow is 1-D and uniform may be over-simplistic, and may constitute an additional source of discrepancies between computation and experiment which then compromises the validation process.

Current expansion tube numerical modelling at UQ adopts a hybrid solution approach (see Fig. 17), whereby only the low pressure acceleration tube and dumptank are modelled two-dimensionally. A radially uniform transient inflow is then defined at the start of the acceleration tube. The inflow is calculated using the 1-D code L1d [42], which models the entire facility including the piston dynamics, and captures the dominant longitudinal wave processes, including their complex interactions. The axisymmetric calculation is performed using the code Eilmer3, developed at UQ by Jacobs et al. [66–68]. Eilmer3 is "an integrated collection of programs for the simulation of transient, compressible flow in two and three spatial dimensions" [67]. The code, which has its origins in the early 1990s under the name 'cns4u', was originally developed for the simulation of reflected shock tunnel and expansion tube impulse facilities. Several aspects of the code make it particularly well-suited to this purpose [67]:

1. It solves the compressible Navier-Stokers equations using an upwinding approach, which can be very effective at capturing the strong shocks associated with these facilities.
2. It has multiple-block capability, which permits a reasonable solution time, using parallel processing, for models which typically are computationally very expensive.
3. It has thermochemistry and finite-rate chemistry capabilities, which are necessary for accurate predictions about the extreme flow processes which occur in these impulse facilities, particularly for superorbital flow conditions (6–15 km/s).

Wheatley et al. [59] argued that the hybrid approach is usually acceptable for two principle reasons. Firstly, the shock tube flow typically has a relatively thin boundary layer on account of its relatively low velocity and high density. Secondly, when the diaphragm separating the test and acceleration tube gases ruptures, the

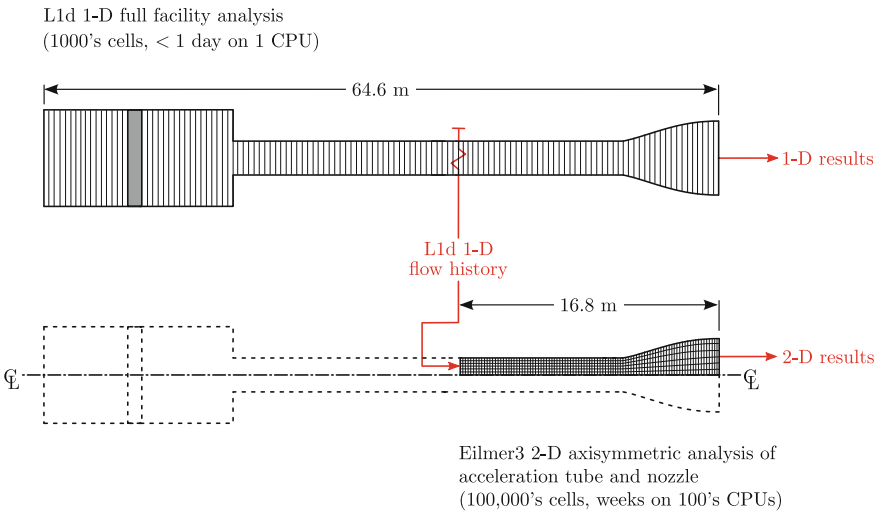

Fig. 17 Schematic diagram of X3 L1d/Eilmer3 CFD hybrid analysis model. Not to scale

downstream portion of the shock-processed test gas, which will eventually be the test flow, is located immediately behind the primary shock, where the boundary layer has only just begun to develop. It is often reasonable therefore to treat the shock-processed test gas as 1-D, and restrict the 2-D axisymmetric calculation to the low pressure acceleration tube and dumptank [59]. This is the approach which has typically been adopted at UQ, for example [54, 69, 70, 71].

Wheatley et al. [59] studied rarefied superorbital flows in UQ's X1 expansion tube (which was decommissioned in 2011). Experimentally measured shock speeds were used to calculate inflow conditions to the acceleration tube. Flow in the acceleration tube and dumptank was then computed using UQ's axisymmetric solver mb_cns (the original precursor to UQ's Eilmer3 code). An earlier study by Wendt et al. [72] on the same facility used a similar approach with mb_cns.

The next phase of studies used the L1d code to calculate the inflow to the shock tube, however these L1d calculations did not include piston dynamics. Instead, the volume between the piston face and the primary diaphragm was modelled as fixed [71]. The driver pressure at primary diaphragm rupture is known; the position of the piston downstream face, and the temperature of the driver gas, are then both adjusted until shock speeds, pressure histories, peak pressures, and pulse duration, satisfactorily match between experiment and the 1-D calculation [71]. This approach extends the reasoning of Wheatley et al. [59] to include a time history of flow properties in the shock tube. It has been used by Jacobs et al. for X3 [71], by Scott [54], McGilvray et al. [73], and Potter et al. [69] for X2, by McGilvray et al. [73] for the Hypervelocity Expansion Tube at the University of Illinois (using the UQ codes), and by Stewart et al. [74] for the RHYFL-X expansion tube concept (also using UQ codes).

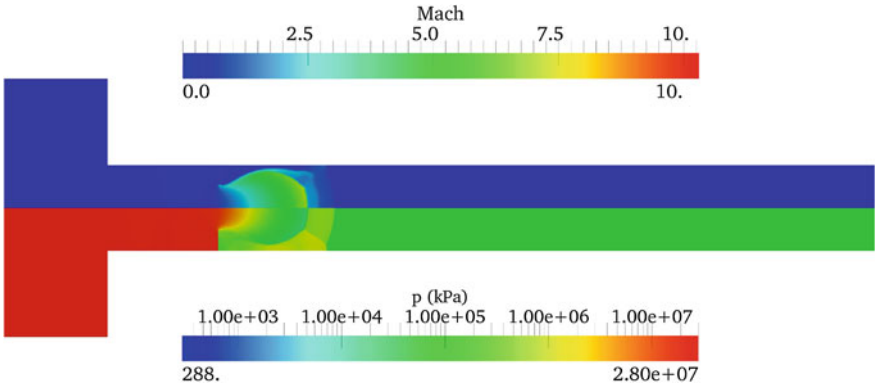

Fig. 18 Axisymmetric CFD simulation of primary diaphragm rupture in UQ's X2 expansion tube [56]

Gollan et al. [75] used a similar approach to simulate flow in X2 operated as a non-reflected shock tube. However, in this instance a more sophisticated L1d model was used, which modelled the full piston dynamics and primary diaphragm rupture. This approach is currently the routine methodology for hybrid simulation of expansion tubes, and has been adopted in recent studies such as Gildfind et al. [45, 76]. However, in order to adequately capture the full transient and spatial characteristics of expansion tube test flows, higher fidelity is required in the modelling of flow processes upstream of the acceleration tube. At the time of writing, piston dynamics is being coded into Eilmer3, and driver gas flow through the rupturing primary diaphragm has already been shown to introduce complex lateral wave disturbances to the driven gas (Fig. 18). Sophisticated high temperature gas models have also been developed for Eilmer3, which include finite rate chemistry [77] and radiation effects [78], which become particularly important for the higher enthalpy conditions (for example, Fig. 19).

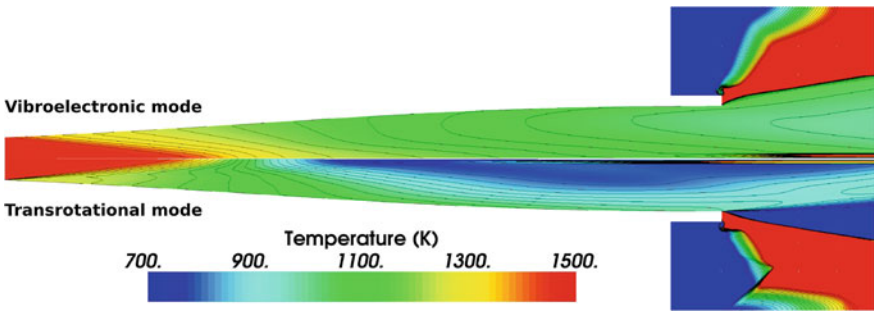

Fig. 19 Temperature contours for nonequilibrium X2 nozzle expansion calculation with Eilmer3 (adapted from [69])

5 The X3 Facility

With support from the Australian Research Council, the development of X3 began in 1994, with targeted dimensions of approximately 65 m total length, and a bore of 182.6 mm [15]. After establishing the feasibility of a compound driver in X2, a much larger two-stage free-piston driver was developed for X3, comprising a 200 kg inner piston, 100 kg outer piston, and a primary diaphragm rupture pressure up to 100 MPa [15]. The commissioning tests for X3 were conducted in January 2001, with the first experiments conducted in May 2001 [29]. In the next few years X3 was used successfully for several aerothermodynamic test campaigns, where simulations typically targeted high enthalpy superorbital speeds [79], for example heat transfer measurements for Titan entry [80].

Several difficulties with the original configuration of X3 did, however, lead to a series of major upgrades to the facility. Principle amongst these was the development of a new single-stage free-piston driver. The original dual-stage arrangement proved complicated to operate, and the requirement to decelerate the outer piston with a buffer arrangement set upper limits on the piston velocity, which in turn limited performance in the tube [79]. The use of a single piston also introduces an area change at the primary diaphragm, and thus provides the corresponding performance benefits this entails. The current experimental configuration of X3 is shown in Fig. 20; various photographs of the upgraded hardware are shown in Fig. 21; the new driver is shown in Fig. 21a.

X3 has been modified to incorporate a contoured Mach 10 nozzle, manufactured from fiberglass using fiber-winding around a mandrel [81]. UQ first applied this technique for the manufacture of contoured Mach 8 and Mach 10 nozzles for the T4 reflected shock tunnel [82]; this technique is also discussed in [51] and [83]. The new nozzle, which has an exit diameter of Ø440 mm, is shown in Fig. 21f; an unexpected consequence of fiberglass construction is light emission through the nozzle during facility operation, characterised as a bright flash during the passing of the hot accelerator gas.

X3's original dumptank was moved to X2 to enable scramjet testing [79], and a new and much larger stainless steel test section was procured for X3 as part of its upgrade (Fig. 21c; foreground). An additional aluminium dumptank, originally

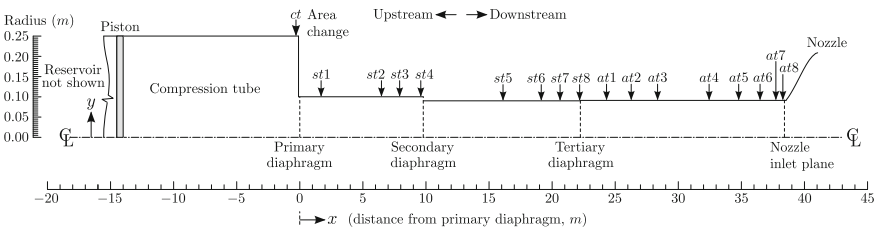

Fig. 20 Geometric layout of X3 expansion tube facility. Longitudinal scale compressed for clarity

Fig. 21 Photographs of X3's upgraded hardware. **a** Ø500 mm bore single stage driver compression tube (protective shielding removed to show capstan with belt drive). **b** Ø500 mm 100.8 kg lightweight piston. **c** Nozzle and test section with 50 mm thick perspex windows installed. **d** Pitot rake instrumented with 15° partial impact cone probes and a Pinckney static pressure probe [76, 85]. **e** Instrumented scramjet in test section (side covers removed). **f** Nozzle flash during facility operation due to flow luminosity [86]

used on the T3 reflected shock tunnel at the Australian National University in Canberra, was also donated to UQ for use with X3; this is attached to the rear of the test section, and approximately doubles the volume of the vacuum chamber (Fig. 21c; background). The new test section provides optical access to experiments, and is fully equipped for scramjet engine experiments. Wide field of view

50 mm thick perspex windows (Fig. 21c) are available for non-specialist optical applications including high speed imaging at up to megahertz frame rates; adaptors permit flexible placement of optical glass for more specialist optics studies such as Schlieren imaging, spectroscopy, holographic interferometry, and so forth.

The new single-stage driver was completed in 2011. Initial commissioning of the driver used a new 200 kg piston. Tuned operation with the piston was achieved with the use of an orifice plate at the driver in combination with helium/argon driver gas mixtures [76]. Flow condition development efforts have initially been directed towards high Mach number scramjet combustion studies. Scramjet testing has been conducted for Mach 10 flight, with 1–2 kPa static pressure, Ø200 mm core flow, and a test time of approximately 1 ms; preliminary characterisation of this test flow is detailed in [76].

While tuned operation of the 200 kg piston has successfully powered the Mach 10 scramjet test flows, higher enthalpy conditions will require higher driver gas sound speeds. As well, tuned operation of the driver at these conditions will require higher piston speeds, which in turn require a lower piston mass. A new lightweight piston has therefore been designed and manufactured (Fig. 21b). The piston is machined from 6061-T6 (the strongest aluminium alloy readily available in Ø500 mm billet), and has been sized for routine operation up to a maximum driver pressure of 40 MPa [84].

An initial commissioning study with the lightweight piston, involving blanked-off testing, was conducted in April 2013. A blanked-off test involves replacing the rupturing primary diagram with thick steel plate; when the piston is launched, instead of the diaphragm rupturing, the piston bounces back and forth. These tests were used to demonstrate the structural integrity of the piston, and to validate 1-D numerical models of X3's driver and piston dynamics [84]. It was found that X3's existing reservoir, at its maximum rated pressure of 14 MPa, has insufficient volume to propel the lightweight piston to the 250–300 m/s maximum speeds required for tuned operation at high driver gas sound speeds. An extension to X3's reservoir has subsequently been commissioned which will increase its volume by 50 %; the reservoir extension is scheduled for delivery and installation in 2015.

In 2014 the facility was used to conduct scramjet engine studies. Initial testing was focused on a 2-D scramjet engine at Mach 10, at a similar dynamic pressure to tests which were previously conducted on the same engine in the T4 RST [87], which approached the limit of T4's capability. Conducting these experiments at a flow condition common to both facilities provides an independent validation of the engine performance as a starting point for high Mach number testing, and in future will be followed by full free stream scramjet testing at Mach 12 and beyond. A new Mach 12 contoured nozzle, with exit Ø647 mm, is currently (2015) under construction and will be used for the Mach 12 scramjet experiments. These scramjet experiments will also require completion of the lightweight piston commissioning process with the upgraded reservoir. In addition to scramjet testing, the new driver and Mach 12 nozzle will also be used for radiation studies of planetary entry flows, using significantly larger models than has previously been possiblewith the UQ facilities.

In addition to the above, instrumentation and data acquisition systems have been improved, and a scramjet hydrogen fuelling system has been developed. Significant design work has also been directed towards improving the reliability and ease of operation of the facility, in order to prepare it for the higher usage rates which will be required into the future.

6 Conclusion

The University of Queensland first began experimenting with free-piston driven expansion tube facilities in the 1980s, and currently has two operational facilities, X2 and X3. Over 2500 shots have been conducted with X2, which has provided a reliable and high performance ground testing capability in support of a broad range of hypersonics studies. X2 has also been the platform for facility development studies, which have included the development of improved free-piston drivers, contoured nozzles, instrumentation, and specialised simulation codes. X3 is a much larger facility than X2, and provides greater capabilities in terms of test time and model size. The improvements achieved with X2 have now been incorporated into X3, which will offer an important ground testing platform for the Australian hypersonics community well into the future.

Acknowledgments The authors wish to thank: Mr F. De Beurs, Mr B. Loughrey, and the rest of the UQ Mechanical Engineering Workshop, for technical support; The Australian Research Council for support and funding; The Queensland Smart State Research Facilities Fund 2005 for support and funding; The Australian Space Research Program and UQ for their funding in support of the "Scramjet-based Access-to-Space Systems" (SCRAMSPACE) project. Many of the advances that have been made, both experimentally and computationally, have come through the PhD and Masters studies of the Group's many students.

References

1. Stalker, R.J.: Isentropic compression of shock tube driver gas. ARS J. **30**, 564 (1960)
2. Paull, A., Stalker, R.J.: Scramjet testing in the T3 and T4 hypersonic impulse facilities. In: Curran, E.T., Murthy, S.N.B. (eds.) Scramjet Propulsion, Progress in Astronautics and Aeronautics, pp. 1–46. AIAA, Reston, Virginia (2000)
3. Stalker, R.J., Morgan, R.G.: The University of Queensland free piston shock tunnel T4: initial operation and preliminary calibration. In: Proceedings of the 4th National Space Engineering Symposium, IEAust, Adelaide (1988)
4. http://hypersonics.mechmining.uq.edu.au/t4. Downloaded 19 Aug 2013
5. Resler, E.L., Bloxsom, D.E.: Very High Mach Number Flows by Unsteady Flow Principles. Cornell University Graduate School of Aeronautical Engineering, Limited Distribution Monograph, Jan 1952
6. Trimpi, R.L.: A preliminary theoretical study of the expansion tube, a new device for producing high-enthalpy short-duration hypersonic gas flows. NASA Technical Report R-133 (1962)

7. Trimpi, R.L.: A theoretical Investigation of Simulation in Expansion Tubes and Tunnels. NASA TR R-243, NASA Langley Research Centre, Langley Station, Hampton, VA (1966)
8. Paull, A., Stalker, R.J., Stringer, I.: Experiments on an expansion tube with a free piston driver. In: Proceedings of the AIAA 15th Aerodynamic Testing Conference, AIAA paper 88-2018, San Diego, CA, 18–20 May 1988
9. Miller, C.G., Jones, J.J.: Development and performance of the NASA Langley Research Center expansion tube/tunnel, a hypersonic-hypervelocity real-gas facility. In: Archer, R.D., Milton, B.E. (eds.) Proceedings of the 14th International Symposium on Shock Waves, pp. 363–373. Sydney, Australia, Aug 1983
10. Miller, C.G.: Operational Experience in the Langley Expansion Tube With Various Test Gases. NASA Technical Memorandum 78637, NASA Langley Research Center, Hampton, VA, Dec 1977
11. Paull, A., Stalker, R.J.: Test flow disturbances in an expansion tube. J. Fluid Mech. **245**, 493–521 (1992)
12. Stalker, R.J.: Recent developments with free piston drivers. In: Kim, Y.W. (ed.) Current topics in shock waves 17th International Symposium on Shock Waves and Shock Tubes, pp 96–105. Bethlehem, PA (1990)
13. Paull, A., Stalker, R.J.: The effect of an acoustic wave as it traverses an unsteady expansion. Phys. Fluids **3**(4), 717–719 (1991)
14. Bakos, R.J., Erdos, J.I.: Options for enhancement of the performance of shock-expansion tubes and tunnels. In: Proceedings of the 33rd Aerospace Sciences Meeting and Exhibit, AIAA 95-0799, Reno, NV, 9–12 Jan 1995
15. Morgan, R.G.: Free-piston driven expansion tubes. In: Ben-Dor, G., Igra, O., Elperin, T. (eds.) Handbook of Shock Waves, vol. 1, pp. 603–622. Academic Press, New York (2001)
16. Bakos, R.J., Morgan, R.G., Tamagno, J.: Effects of oxygen dissociation on hypervelocity combustion experiments. In: Proceedings of the AIAA 17th Aerospace Ground Testing Conference, AIAA-92-3964, Nashville, TN, 6–8 July 1992
17. Jones, J.J.: Some performance characteristics of the LRC 3-3/4-inch pilot expansion tube using an unheated hydrogen driver. In: Proceedings of the Fourth Hypervelocity Techniques Symposium, pp 7–26. Arnold Engineering Development Center, Arnold Air Force Station, Tennessee, 15–16 Nov 1965
18. Spurk, J.H.: Design, operation, and preliminary results of the BLR expansion tube. In: Proceedings of the Fourth Hypervelocity Techniques Symposium, pp. 111–144. Arnold Engineering Development Center, Arnold Air Force Station, Tennessee, 15–16 Nov 1965
19. Norfleet, G.D., Lacey, J.J., Whitfield, J.D.: Results of an experimental investigation of the performance characteristics of an expansion tube. In: Proceedings of the Fourth Hypervelocity Techniques Symposium, pp. 49–110. Arnold Engineering Development Center, Arnold Air Force Station, Tennessee, 15–16 Nov 1965
20. Miller, C.G.: Operational experience in the Langley expansion tube with various test gases. NASA Technical Memorandum 78637 (1977)
21. Jacobs, P.A.: Numerical simulation of transient hypervelocity flow in an expansion tube. ICASE Interim Report 20/NASA Contractor Report 189601, Langley Research Center, Hampton, Virginia, Jan 1992
22. Neely, A.J., Stalker, R.J., Paull, A.: High enthalpy, hypervelocity flows of air and argon in an expansion tube. Aeronaut. J. **95**(946), 175–186 (1991)
23. Jacobs, P.A.: Numerical simulation of transient hypervelocity flow in an expansion tube. Comput. Fluids **23**(1), 77–101 (1994)
24. Henshall, B.D.: The use of multiple diaphragms in shock tubes. A.R.C. Technical Report C. P. No. 291, Ministry of Supply, Aeronautical Research Council (1956)
25. Stalker, R.J., Plumb, D.L.: Diaphragm-type shock tube for high shock speeds. Nature **218** (5143), 789–790 (1968)
26. Morgan, R.G.: A review of the use of expansion tubes for creating superorbital flows. In: Proceedings of the 35th Aerospace Sciences Meeting and Exhibit, AIAA 97-0279, Reno, NV, 6–10 Jan 1997

27. Morgan, R.G., Stalker, R.J.: Double diaphragm driven free piston expansion tube. In: Proceedings of the 18th International Symposium on Shock Waves, Sendai, Japan, 21–26 July 1991
28. Neely, A.J., Morgan, R.G.: The superorbital expansion tube concept, experiment and analysis. Aeronaut. J. **98**, 97–105 (1994)
29. Scott, M.P., Morgan, R.G., Jacobs, P.A.: A new single stage driver for the X2 expansion tube. In: Proceedings of the 43rd AIAA Aerospace Sciences Meeting and Exhibition, AIAA-2005-697, Reno, Nevada, 10–13 Jan 2005
30. Doolan, C.J., Morgan, R.G.: A two-stage free-piston driver. Shock Waves **9**(4), 239–249 (1999)
31. Doolan, C., Morgan, R.G.: Test-time optimization of a large scale hypervelocity expansion tunnel. In: Proceedings of the Eighth National Space Engineering Symposium, The Institution of Engineers, Australia, Brisbane, 20–21 Sept 1993
32. Eichmann, T.N., McIntyre, T.J., Bishop, A.I., Vakata, S., Rubinsztein-Dunlop, H.: Three-dimensional effects on line-of-sight visualization measurements of supersonic and hypersonic flow over cylinders. Shock Waves **16**, 299–307 (2007)
33. McIntyre, T.J., Lourel, I., Eichmann, T.N., Morgan, R.G., Jacobs, P.A., Bishop, A.I.: Experimental expansion tube study of the flow over a toroidal ballute. J. Spacecraft Rockets **41** (5), 716–725 (2004)
34. Littleton, B.N., Bishop, A.I., McIntyre, T.J., Barker, P.F., Rubinsztein-Dunlop, H.: Flow tagging velocimetry in a superorbital expansion tube. Shock Waves **10**, 225–228 (2000)
35. Hayne, M.J., Mee, D.J., Gai, S.L., McIntyre, T.J.: Boundary layers on a flat plate at sub- and superorbital speeds. J. Thermophys. Heat Transfer **21**(4), 772–779 (2007)
36. Higgins, C., Inger, G.R., Morgan, R., Eichmann, T., McIntyre, T.: Shock standoff on hypersonic blunt bodies in multi-temperature ionizing nonequilibrium gas flows. In: Proceedings of the 8th AIAA/ASME Joint Thermophysics and Heat Transfer Conference, St Louis, Missouri, 24–26 June 2002
37. Eichmann, T.N.: Radiation measurements in a simulated Mars atmosphere. PhD Thesis, School of Mathematics and Physics, The University of Queensland, Brisbane, Australia (2012)
38. Jacobs, C.M.: Radiation in low density hypervelocity flows. PhD Thesis, School of Mechanical and Mining Engineering, The University of Queensland, Brisbane, Australia (2011)
39. Brandis, A.M., Morgan, R.G., McIntyre, T.J.: Analysis of nonequilibrium CN radiation encountered during Titan atmospheric entry. AIAA J. Thermophys. Heat Transfer **25**(4), 493–499 (2007)
40. McGilvray, M., Morgan, R., Jacobs, P.: Scramjet experiments in an expansion tunnel: evaluated using a quasi-steady analysis technique. AIAA J. **48**(8), 1635–1646 (2010)
41. Gildfind, D.E., Morgan, R.G., McGilvray, M., Jacobs, P.A., Stalker, R.J., Eichmann., T.N.: Free-piston driver optimisation for simulation of high Mach number scramjet flow conditions. Shock Waves **21**(6), 559–572 (2011)
42. Jacobs, P.A.: Quasi-one-dimensional modelling of a free-piston shock tunnel. AIAA J. **32**(1), 137–145 (1994)
43. Stalker, R.J.: A study of the free-piston shock tunnel. AIAA J. **5**(12), 2160–2165 (1967)
44. Itoh, K., Ueda, S., Komuro, T., Sato, K., Takahashi, M., Myajima, H., Tanno, H., Muramoto, H.: Improvement of a free piston driver for a high-enthalpy shock tunnel. Shock Waves **8**(4), 215–233 (1998)
45. Gildfind, D.E., Morgan, R.G., Jacobs, P.A., McGilvray, M.: Production of High-Mach-Number scramjet flow conditions in an expansion tube. AIAA J. **52**(1), 162–177 (2014)
46. Porat, H., Zander, F., Morgan, R.G., McIntyre, T.J.: Emission spectroscopy of a mach disk at Titan atmospheric entry conditions. In: Proceedings of the 29th International Symposium on Shock Waves, University of Wisconsin, Madison, 14–19 July 2013

47. Sheikh, U.A., Jacobs, C., Laux, C.O., Morgan, R.G., McIntyre, T.J.: Measurements of radiating flow fields in the vacuum ultraviolet. In: Proceedings of the 29th International Symposium on Shock Waves, University of Wisconsin, Madison, 14–19 July 2013
48. Zander, F., Morgan, R.G., Sheikh, U., Buttsworth, D.R., Teakle, P.R.: Hot-wall reentry testing in hypersonic impulse facilities. AIAA J. **51**(2), 476–484 (2013)
49. James, C.M., Gildfind, D.E., Morgan, R.G., McIntyre, T.J.: Working towards simulating gas giant entry radiation in an expansion tube. In: Proceedings of the 29th International Symposium on Shock Waves, University of Wisconsin, Madison, 14–19 July 2013
50. Gildfind, D.E., James, C.M., Morgan, R.G.: Free-piston driver performance characterisation using experimental shock speeds through helium. Shock Waves, **25**(1), 169–176 (2015)
51. Bakos, R.J., Calleja, J.F., Erdos, J.I., Auslender, A.H., Sussman, M.A., Wilson, G.J.: Design, calibration and analysis of a tunnel mode of operation for the hypulse facility. In: Proceedings of the 19th AIAA Advanced Measurement and Ground Testing Technology Conference, AIAA 96-2194, New Orleans, LA, 17–20 June 1996
52. Stewart, B.S., Jacobs, P.A., Morgan, R.G.: The starting process of an expansion tube nozzle. In: 23rd International Symposium on Shock Waves, The University of Texas at Arlington, USA, 23–27 July 2001
53. Chue, R.S.M., Bakos, R.J., Tsai, C.-Y., Betti, A.: Design of a shock-free expansion tunnel nozzle in hypulse. Shock Waves **13**(4), 261–270 (2003)
54. Scott, M.P.: Development and modelling of expansion tubes. PhD Thesis, Centre for Hypersonics, Department of Mechanical Engineering, University of Queensland, Brisbane, Australia (2006)
55. Craddock, C.S.: Computational optimization of scramjets and shock tunnel nozzles. PhD Thesis, Department of Mechanical Engineering, The University of Queensland, Brisbane, Australia (1999)
56. Gildfind, D.: Development of high total pressure scramjet flow conditions using the X2 expansion tube. PhD Thesis, Division of Mechanical Engineering, School of Engineering, The University of Queensland, Brisbane, Australia (2012)
57. McGilvray, M., Jacobs, P.A., Morgan, R.G., Gollan, R.J., Jacobs, C.M.: Helmholtz resonance of pitot pressure measurements in impulsive hypersonic test facilities. AIAA J. **47**(10), 2430–2439 (2009)
58. Chiu, H.S., Mee, D.J.: Modified bar gauges. Research Report Number 2003/22, Division of Mechanical Engineering, The University of Queensland (2003)
59. Wheatley, V., Chiu, H.S., Jacobs, P.A., Macrossan, M.N., Mee, D.J., Morgan, R.G.: Rarefied, superorbital flows in an expansion tube. Int. J. Numer. Meth. Heat Fluid Flow **14**(4), 512–537 (2004)
60. Hillier, R., Boyce, R.R., Creighton, S.A., Fiala, A., Jackson, A.P., Mallinson, S.G., Sheikh, A. H., Soltani, S., Williams, S.: Development of some hypersonic benchmark flows using CFD and experiment. Shock Waves **12**(5), 375–384 (2003)
61. Roy, C.J., Oberkampf, W.L., McWherter-Payne, M.A.: Verification and validation for laminar hypersonic flow fields, Part 2: validation. AIAA J. **41**(10), 1944–1954 (2003)
62. Anderson, G., Kumar, A., Erdos, J.: Progress in hypersonic combustion technology with computation and experiment. In: AIAA Second International Aerospace Planes Conference, AIAA-90-5254, Orlando, FL, 29–31 Oct 1990
63. Anderson, G.Y., McClinton, C.R., Weidner, J.P.: Scramjet performance. In: Curran, E.T., Murthy, S.N.B. (eds.) Scramjet Propulsion, Progress in Astronautics and Aeronautics, pp. 369–446. AIAA, Reston, Virginia (2000)
64. Candler, G.V., Nompelis, I.: CFD validation for hypersonic flight: real gas flows. In: Proceedings of the 40th AIAA Aerospace Sciences Meeting and Exhibit, RTO-TR-AVT-007-V3/AIAA 2002-0434, Reno, NV, 14–17 Jan 2002
65. Marvin, J.G.: A CFD Validation Roadmap for Hypersonic Flows. NASA Technical Memorandum 103935, Ames Research Center, Moffett Field, California (1992)

66. Jacobs, P.A., Gollan, R.J.: The Eilmer3 Code: User Guide and Example Book. Mechanical Engineering Report 2008/07, Department of Mechanical and Mining Engineering, The University of Queensland (2009)
67. Jacobs, P.A., Gollan, R.J., Denman, A.J., O'Flaherty, B.T., Potter, D.F., Petrie-Repar, P.J., Johnston, I.A.: Eilmer's Theory Book: Basic Models for Gas Dynamics and Thermochemistry. Mechanical Engineering Report 2010/09, Department of Mechanical and Mining Engineering, The University of Queensland (2010)
68. Gollan, R.J., Jacobs, P.A.: About the formulation, verification and validation of the hypersonic flow solver Eilmer. Int. J. Numer. Meth. Fluids **73**, 19–57 (2013)
69. Potter, D.F., Gollan, R.J., Eichmann, T., McIntyre, T.J., Morgan, R.G., Jacobs, P.A.: Simulation of CO2-N2 expansion tunnel flows for the study of radiating shock layers. In: Proceedings of the 46th AIAA Aerospace Sciences Meeting and Exhibit, AIAA 2008-1280, Reno, Nevada, 7–10 Jan 2008
70. Morgan, R.G., McIntyre, T.J., Jacobs, P.A., Buttsworth, D.R., Macrossan, M.N., Gollan, R.J., Capra, B.R., Brandis, A.M., Potter, P., Eichmann, T., Jacobs, C.M., McGilvray, M., van Diem, D., Scott, M.P.: Impulse facility simulation of hypervelocity radiating flows. In: Proceedings of the 2nd International Workshop on Radiation of High Temperature Gases in Atmospheric Entry, 6–8 Sept, Rome, Italy. ESA Publication, Noordwijk, The Netherlands, Nov 2006
71. Jacobs, P.A., Silvester, T.B., Morgan, R.G., Scott, M.P., Gollan, R.G., McIntyre, T.J.: Superorbital expansion tube operation: estimates of flow conditions via numerical simulation. In: Proceedings of the 43rd AIAA Aerospace Sciences Meeting, AIAA-2005-0694, Reno, NV, 10–13 Jan 2005
72. Wendt, M., Macrossan, M., Jacobs, P., Mee, D.: Pilot study for a rarefied hypervelocity test facility. In: Proceedings of the 13th Australasian Fluid Mechanics Conference, Monash University, Melbourne, Australia, 13–18 Dec 1998
73. McGilvray, M., Austin, J.M., Sharma, M., Jacobs, P.A., Morgan, R.G.: Diagnostic modelling of an expansion tube operating condition. Shock Waves **19**(1), 59–66 (2009)
74. Stewart, B., Morgan, R.G., Jacobs, P.A., Hayne, M.: Flow establishment in large-scale high-performance expansion tubes. In: Proceedings of the AIAA/AAAF 11th International Space Planes and Hypersonic Systems and Technologies Conference, Paper No. 5239, Orleans, France, 29 Sept–4 Oct 2002
75. Gollan, R.J., Jacobs, C.M., Jacobs, P.A., Morgan, R.G., McIntyre, T.J., Macrossan, M.N., Buttsworth, D.R., Eichmann, T.N., Potter, D.F.: A simulation technique for radiating shock tube flows. In: Klauss, H., Seiler, F. (eds.) Proceedings of the 26th International Symposium on Shock Waves, pp. 465–470. Göttingen, Germany, 15–20 July 2007
76. Gildfind, D.E., Sancho, J., Morgan, R.G.: High Mach number scramjet test flows in the X3 expansion tube. In: Proceedings of the 29th International Symposium on Shock Waves, University of Wisconsin-Madison, Memorial Union, 14–19 July 2013
77. Gollan, R.J.: The computational modelling of high-temperature gas effects with application to hypersonic flows. PhD Thesis, Division of Mechanical Engineering, School of Engineering, The University of Queensland, Brisbane, Australia (2008)
78. Potter, D.: Modelling of radiating shock layers for atmospheric entry at Earth and Mars. PhD Thesis, Division of Mechanical Engineering, School of Engineering, The University of Queensland, Brisbane, Australia (2011)
79. McGilvray, M.: The use of expansion tube facilities for scramjet testing. PhD Thesis, Centre for Hypersonics, Department of Mechanical Engineering, The University of Queensland, Brisbane, Australia (2008)
80. Capra, B.R., Morgan, R.G.: Radiative and total heat transfer measurements to a Titan explorer model. J. Spacecraft Rockets **49**(1) (2012)
81. Davey, M.G.: A hypersonic nozzle for the X3 expansion tube. Bachelor of Engineering Thesis, Department of Mechanical Engineering, The University of Queensland, Brisbane, Australia (2006)
82. Jacobs, P.A., Stalker, R.J.: Design of axisymmetric nozzles for reflected shock tunnels. Report 1/89, Department of Mechanical Engineering, University of Queensland (1989)

83. Hass, N.E., Shih, A.T., Rogers, R.C.: Mach 12 and 15 scramjet test capabilities of the hypulse shock-expansion tunnel. In: Proceedings of the 43rd AIAA Aerospace Sciences Meeting and Exhibit, AIAA 2005-690, Reno, Nevada, 10–13 Jan 2005
84. Gildfind, D.E., Morgan, R.G., Sancho, J.: Design and commissioning of a new lightweight piston for the X3 expansion tube. In: Proceedings of the 29th International Symposium on Shock Waves, University of Wisconsin-Madison, Memorial Union, 14–19 July 2013
85. Pinckney, S.Z.: A short static-pressure probe design for supersonic flow. NASA TN D-7978 (1975)
86. Zander, F.: Personal communication (2012)
87. McGilvray, M., Kirchhartz, R., Jazra, T.: Comparison of Mach 10 scramjet measurements from different impulse facilities. AIAA J. **48**(8), 1647–1651 (2010)

Author Biographies

David E. Gildfind Centre for Hypersonics, School of Mechanical and Mining Engineering, The University of Queensland, Brisbane, Australia; David Gildfind's research is concerned with the development of hypersonic impulse facilities. His main efforts have been directed towards optimising free-piston driver operation, expansion tube flow condition development, and test flow characterisation. David graduated as an aerospace engineer from RMIT University in 2001, and worked for a number of years on various aircraft platforms in Australia and overseas. He later undertook his PhD and several years of post-doctoral work in hypersonics at the University of Queensland (UQ), and is now a lecturer within UQ's School of Mechanical and Mining Engineering.

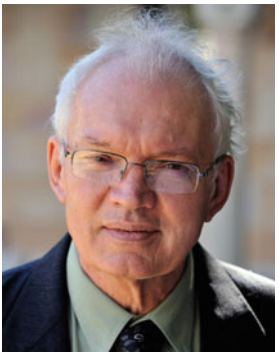

Richard G. Morgan Centre for Hypersonics, School of Mechanical and Mining Engineering, The University of Queensland, Brisbane, Australia; Richard Morgan has been the Director of the Centre for Hypersonics at The University of Queensland since its inception in 1997, and lectures in the School of Mechanical and Mining Engineering. Richard developed the superorbital expansion tube concept, which enables flows at speeds in excess of 50,000 km/h to be generated in the laboratory. He is an expert in modelling and testing the influences of radiation from the hot flows that occur in the bow waves of vehicles entering the atmospheres of the earth, other planets and moons. He has collaborative research programs with NASA, ESA, Oxford University, Ecole Centrale (Paris) and AOARD in radiating flows, as well as continuing Australian Research Council (ARC) support in this area since 1990. He was involved as a flight team member in the 2010 airborne observation of the Japanese 'Hayabusa' asteroid sample return mission, for which he was a co-recipient of the NASA Ames 'honour' award for 2010. He received his undergraduate and postgraduate degrees from The University of Oxford.

Peter A. Jacobs Centre for Hypersonics, School of Mechanical and Mining Engineering, The University of Queensland, Brisbane, Australia; Peter Jacobs has worked on shock tube and expansion tube simulations for more than 25 years. His work on expansion tubes started at NASA Langley Research Center, following discussions with Charles Miller, Judy Shinn and Bob Trimpi. Since then, much of what he has learned about the gas dynamic processes in these machines has been encoded into a set of flow simulation programs that are maintained by the Compressible Flow CFD group at The University of Queensland. (See http://cfcfd.mechmining.uq.edu.au) He is a graduate of The University of Queensland and spends most of his days teaching or thinking about computation and gas dynamics.